

Progress report for the 2007 SCEC project  
**Continued analysis of small-scale strain patterns associated  
with southern California earthquakes**

Thorsten W. Becker  
University of Southern California, Los Angeles

March 11, 2008

## **Project objective**

This report is for the last year of funding for a three year effort to understand the spatial scales of seismic strain release in southern California as imaged by the summation of focal mechanisms. We are able to show that there are persistent, small-scale, deterministic features across magnitude ranges, and that those patterns are likely related to fault geometries.

The project has provided funding for graduate student Iain Bailey. We have now submitted an initial paper that describes fundamental methods and a subset of our results which are summarized below. We also comment on related work on strain summation along the whole plate boundary.

Resulting publications and presentations within project years 2006 and 2007:

- Bailey, I., Becker, T. W., and Ben-Zion, Y.: Patterns of co-seismic strain computed from southern California focal mechanisms. Submitted to *Geophys. J. Int.*, 2008. Available online at <http://geodynamics.usc.edu/~becker/preprints/bbb08.pdf>.
- Platt, J. P., Kaus, B. J. P., and Becker, T. W.: The San Andreas Transform system and the tectonics of California: An alternative approach. To be submitted to *Earth Planet. Sci. Lett.*
- For the main project involving Bailey and Ben-Zion: Two SCEC presentations, two SSA presentations, one AGU presentation, one Mathematical Geophysics presentation.

## **Main project summary**

Geometrical properties of an earthquake population can be described by summation of seismic potency tensors that provide a strain-based description of earthquake focal mechanisms. Bailey *et al.* (2008) apply this method to  $\sim 170,000$  potency tensors for  $0 < M_L \leq 5$  southern California earthquakes recorded between January 1984 and June 2003. We compare summed tensors for populations defined by faulting region and earthquake magnitude in order to investigate the relation between earthquake characteristics, tectonic domains and fault-related length scales. We investigate spatial scales ranging from  $\sim 1$ –270 km and use the results to identify systematic differences between seismic behaviour for different faults and different regions. Our results show features that are indicative of both scale-invariant and scale-dependent processes. On the largest scale the overall potency tensor summation for southern California  $0 < M_L \leq 5$  earthquakes over  $\sim 20$  years corresponds closely to a double-couple mechanism with slip direction parallel to plate

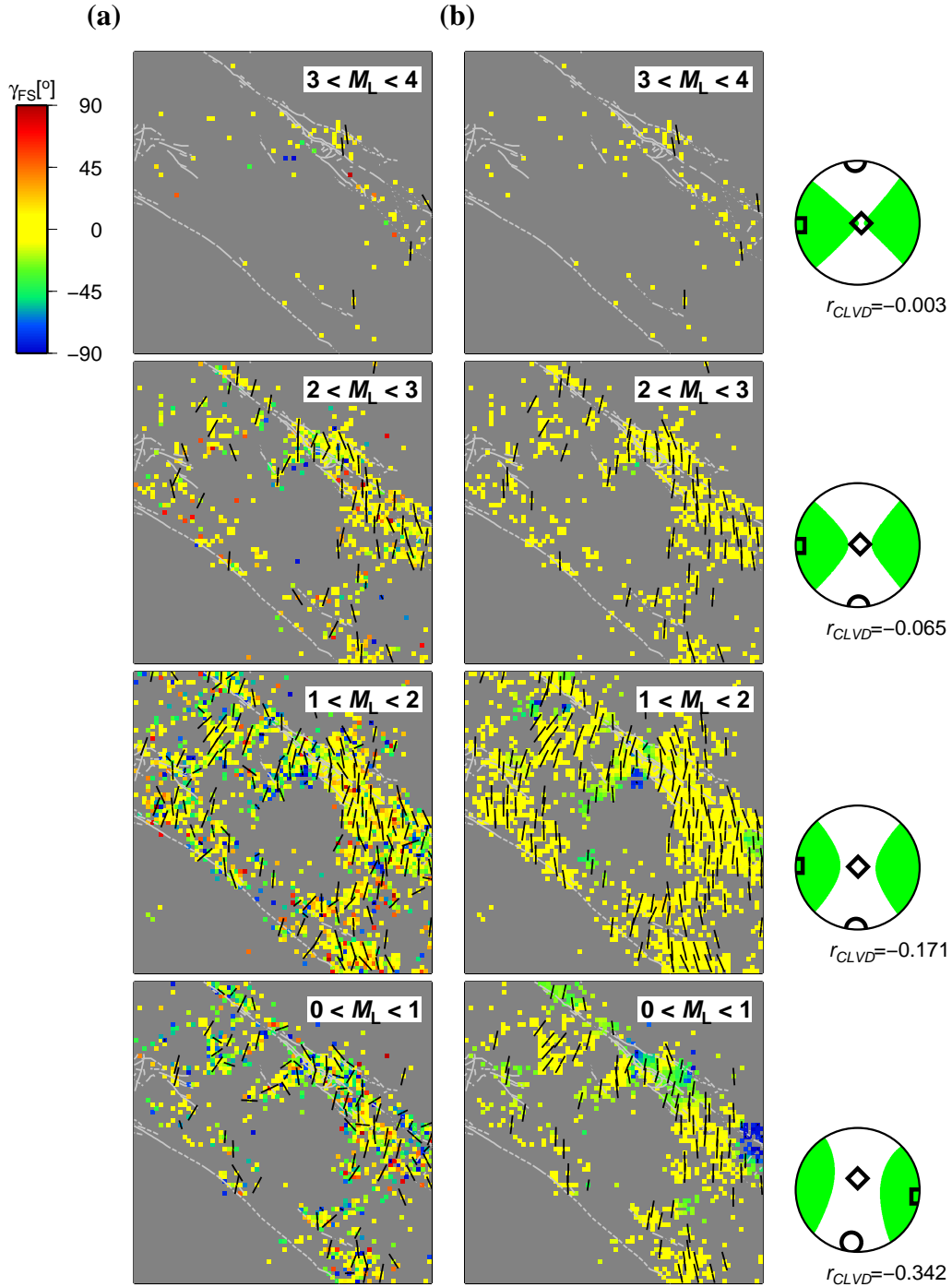


**Figure 1:** The (a) gridded summation and (b) quality adaptive summation results of  $P_{ij}^{SM}$  for part of the San Jacinto (northern section of SJ in Figure 2) over four magnitude bins displayed in terms of dominant fault style (colours) and P-axis azimuths (bars). Source mechanism summations for all earthquakes in the region are shown by beachball plots and  $r_{CLVD}$  values to the right. (From Bailey *et al.*, 2008, see this paper for details.)

motion. The summed tensors and derived quantities for the different regions show clear persistent variations that are related to the dominant tectonic regime of each region. Significant differences between the non-double-couple components of the summed tensors, which we relate to fault heterogeneity, indicate systematic differences in deformation associated with earthquake populations from different fault zones or different magnitude ranges. We find an increase in heterogeneity associated with populations of smaller earthquakes, even when corrected for quality, and regions where faulting deviates strongly from the overall sense of deformation. The results imply overall organisation of the earthquake characteristics into domains that are controlled to first order by geometrical properties of the largest fault and plate motion. Smaller scale organisations are related to local variations in the orientation, complexity and size of faults.

### Method: Summed Potency Tensors

For a population of  $N$  earthquakes, the combined potency tensor can be calculated by a potency tensor summation,

$$P_{ij}^{TOT} = \sum_{k=1}^N P_{ij}^{(k)}. \quad (1)$$

The associated inelastic strain for a volume including the earthquakes,  $V$ , is given by  $P_{ij}^{TOT}/(V)$ , and the mean rate of deformation due to the earthquakes over a time period,  $\Delta t$ , is given by  $P_{ij}^{TOT}/(V\Delta t)$ . Kostrov (1974) defines these quantities in terms of  $M_{ij}$ , and uses a factor of  $1/(2\mu)$ , where  $\mu$  is rigidity, to account for elastic properties of  $V$ . In a population with a wide range of earthquake sizes,  $P_{ij}^{TOT}$  is likely to be dominated by the largest earthquakes, so advantages provided by a large number of small events, such as the lesser influence of outliers and wide spatial sampling, are somewhat diminished. It is therefore also useful to examine summations of source mechanism tensors.

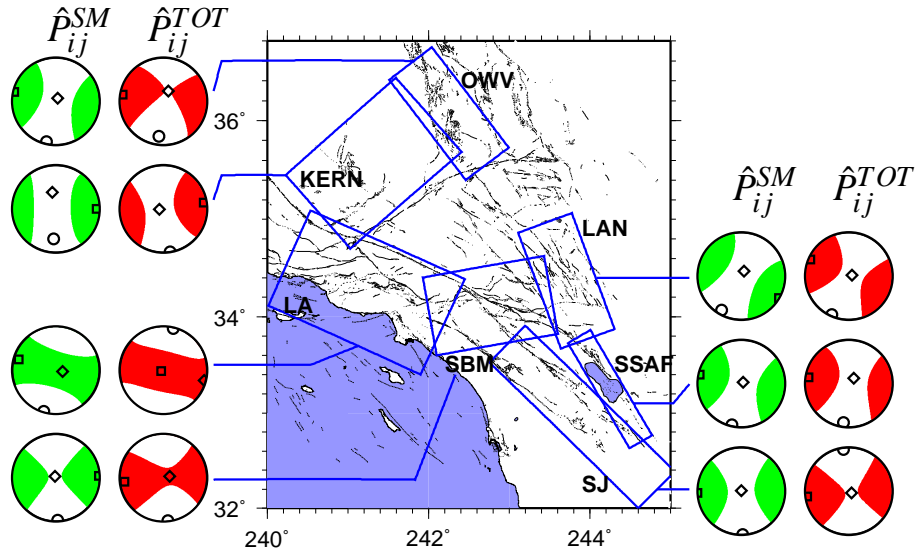
### Results for San Jacinto fault trifurcation region magnitude bins

As an example result from Bailey *et al.* (2008), we show summations divided into magnitude subsets in terms of rake angle  $\gamma_{FS}$  and CLVD component,  $r_{CLVD}$ , in Figure 1. We see no clear differences between spatial patterns of the orientations for different magnitude bins (*cf.* Amelung & King, 1997), and robust non-strike-slip features are found at all magnitude bins for which there are data. This implies that the same length-scales control earthquake behaviour over a range of at least four magnitude units. In Bailey *et al.* (2008) we show that this holds true even when correcting for quality.

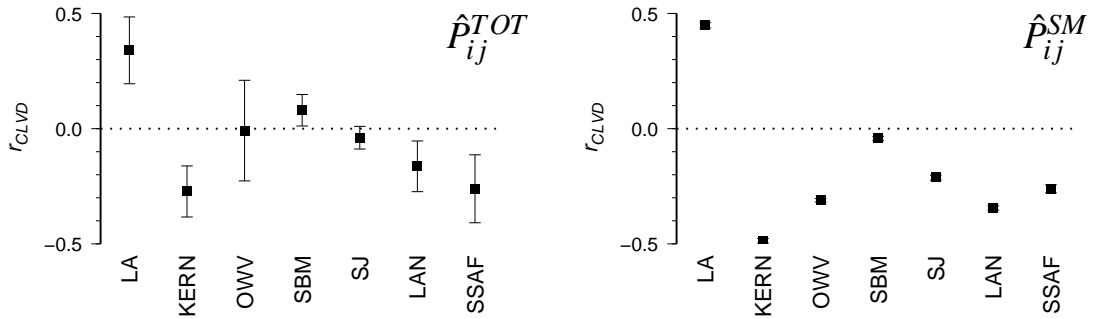
### Results for magnitude bins separated into tectonic regions

Figure 2a from Bailey *et al.* (2008) shows the results of scaled and normalized potency tensor summations for each of the seven regional subsets of our catalogue. In all regions, the orientations of strain axes for the two summation types are reasonably consistent with each other, although this consistency is not as strong in some regions (e.g. KERN and OWV) as for the entire southern California summations. In all results except  $\hat{P}_{ij}^{TOT}$  for the LA region, the B-axis is the most vertical

(a)



(b)



**Figure 2:** (a) Summations of potency tensors and source mechanism tensors for seven tectonically defined regions, using earthquakes in the range  $0 < M_L \leq 5$ . The radii of the beachball plots are equal, such that these represent the normalised tensors,  $\hat{P}_{ij}^{TOT}$  and  $\hat{P}_{ij}^{SM}$  for each bin. P, T and B-axis orientations are overlain (b) Values of  $r_{CLVD}$  for the different regions. Error bars show the 95% confidence limits predicted by bootstrap analysis. For the source mechanism summations, these limits are all smaller than the symbol size. (From Bailey *et al.*, 2008, see this paper for details).

axis, indicating a dominance of strike-slip deformation at these  $\sim 50 - 250$  km scales. Since the B-axes are vertical, the significant variation in the azimuths of the P and T axes accounts for the angular differences between the regions, which are in general much larger than those of neighboring magnitude bins. For example, the T-axis of  $\hat{P}_{ij}^{TOT}$  in the neighboring regions LAN and SBM have azimuths differing by  $\sim 30^\circ$ , compared to the  $2.4^\circ$  azimuthal difference in T-axes of the  $\hat{P}_{ij}^{TOT}$  summations for  $1 < M_L \leq 2$  and  $2 < M_L \leq 3$  bins. It appears from visual inspection of the axes and fault map that the P and T axis orientations are consistently close to  $45^\circ$  from the

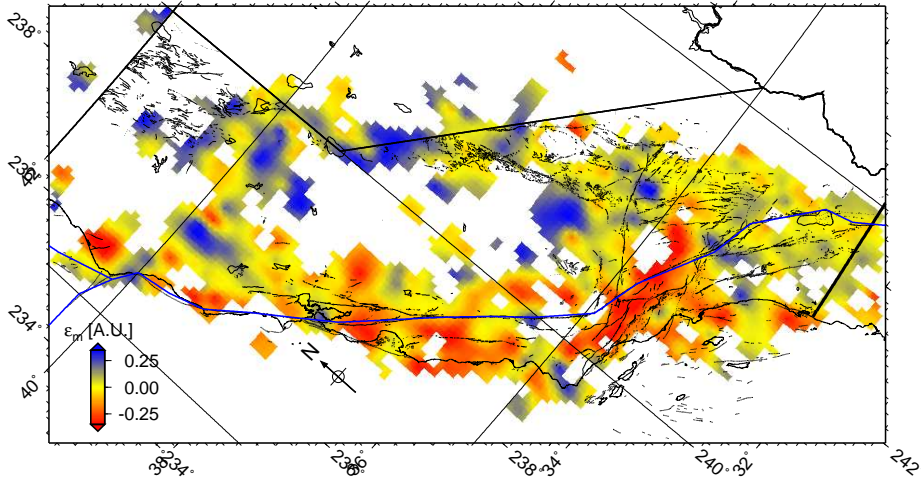


**Figure 3:** Mean (dilatational) horizontal strain as inferred from normalized Kostrov summation of our merged California catalog (see Platt *et al.*, 2008). Red and blue regions correspond to crustal thickening and thinning, respectively, and we show only well constrained regions.

dominant fault strikes of each region. However, despite the agreement of the southern California summations with plate motion directions, few of these smaller regions have P and T axes aligned with those of the entire region.

Figure 2b shows that all regions except SBM have a larger CLVD component than that of the entire region in the source mechanism summation. For the potency tensor summations, the CLVD components are in general smaller, but based on the error bars we can be confident that they are non-zero for the regions LA, KERN, LAN and SSAF. Of these, LA is the only case where  $r_{CLVD}$  is positive, implying that the small positive CLVD component of  $\hat{P}_{ij}^{TOT}$  for the entire southern California region results largely from reverse faulting in the Los Angeles region. The other regions have a greater tendency for normal faulting, though the higher  $r_{CLVD}$  values for  $\hat{P}_{ij}^{SM}$  suggest that this tendency is greater for smaller magnitude earthquakes. Larger confidence intervals for  $r_{CLVD}$  of  $\hat{P}_{ij}^{TOT}$  reflect a sensitivity to a small number of large earthquakes in these summations.

Further results and implications are discussed in Bailey *et al.* (2008).

## Results from related work

John Platt (USC), Boris Kaus (USC and ETHZ), and Becker have developed a thin-sheet description of the San Andreas fault as a weak zone that is terminated by zero shear stress boundary conditions at its northern and southern triple junction termini (Platt *et al.*, 2008). This model predicts second-order regions of vertical motions that are directly associated with the plate boundary and, if true, will be superimposed on the overall shear strain due to the transform.

In southern California, the Platt *et al.* (2008) thin sheet model predicts crustal thickening consistent with the tectonics of the Transverse Ranges and Borderland region, as well as thinning in the Salton Sea and Death Valley area. Moreover, the dilatational component of the horizontal strain-rate field that can be imaged a normalized Kostrov summation of a joint catalog (Figure 3) is also consistent with the model predictions. The combined catalog used for Figure 3 is a merged version of 1964 – 01/2008 USGS NCSN (2008) and the 1975 - 2000 Hauksson (2000) catalogs.

## References

- Amelung, F. & King, G. C. P., 1997. Large-scale tectonic deformation inferred from small earthquakes. *Nature*, **386**, 702–705.
- Bailey, I., Becker, T. W. & Ben-Zion, Y., 2008. Patterns of co-seismic strain computed from southern California focal mechanisms. *Geophys. J. Int.*, **submitted**. Available online at <http://geodynamics.usc.edu/~becker/preprints/bbb08.pdf>.
- Hauksson, E., 2000. Crustal structure and seismicity distribution adjacent to the Pacific and North America plate boundary in southern California. *J. Geophys. Res.*, **105**, 13875–13903.
- Kostrov, B. V., 1974. Seismic moment and energy of earthquakes and seismic flow of rock. *Phys. Solid Earth*, **1**, 23–40.
- Platt, J. P., Kaus, B. J. P. & Becker, T. W., 2008. The San Andreas transform system and the tectonics of California: an alternative approach. *Earth Planet. Sci. Lett.*, **to be submitted**.
- USGS NCSN, 2008. Usgs ncsn catalog. Northern California Earthquake Data Center, Berkeley CA. Available online at <http://www.ncedc.org/ncedc/catalog-search.html>, accessed January 2008.